Quantifying differential rock-uplift rates via stream profile analysis

Eric Kirby* Institute for Crustal Studies, University of California, Santa Barbara, California 93106, USA
Kelin Whipple Department of Earth, Atmospheric and Planetary Sciences, Massachusetts Institute of Technology, Cambridge, Massachusetts 02139, USA

ABSTRACT

Despite intensive research into the coupling between tectonics and surface processes, our ability to obtain quantitative information on the rates of tectonic processes from topography remains limited due primarily to a dearth of data with which to test and calibrate process rate laws. Here we develop a simple theory for the impact of spatially variable rock-uplift rate on the concavity of bedrock river profiles. Application of the analysis to the Siwalik Hills of central Nepal demonstrates that systematic differences in the concavity of channels in this region match the predictions of a stream power incision model and depend on the position and direction of the channel relative to gradients in the vertical component of deformation rate across an active fault-bend fold. Furthermore, calibration of model parameters from channel profiles argued to be in steady state with the current climatic and tectonic regime indicates that (1) the ratio of exponents on channel drainage area and slope (m/n) is ~0.46, consistent with theoretical predictions; (2) the slope exponent is consistent with incision either linearly proportional to shear stress or unit stream power ($n = 0.66$ or $n = 1$, respectively); and (3) the coefficient of erosion is within the range of previously published estimates (mean $K = 4.3 \times 10^{-4}$ $m^{0.2}/yr$). Application of these model parameters to other channels in the Siwalik Hills yields estimates of spatially variable erosion rates that mimic expected variations in rock-uplift rate across a fault-bend fold. Thus, the sensitivity of channel gradient to rock-uplift rate in this landscape allows us to derive quantitative estimates of spatial variations in erosion rate directly from topographic data.

Keywords: geomorphology, stream gradient, fluvial erosion, neotectonics, Siwalik Hills.

INTRODUCTION

A principal goal of tectonic geomorphology is to extract information regarding the rates and patterns of active deformation directly from landscape topography. In tectonically active regions, the bedrock channel network dictates critical relationships among relief, elevation, and denudation rate (Howard, 1994; Howard et al., 1994; Whipple et al., 1999). Consequently, analysis of the longitudinal profiles of channels provides a promising avenue of exploration of these relationships (Hack, 1957), and much recent research has focused on the quantitative description of bedrock channel forms and processes (e.g., Tinkler and Wohl, 1998). However, our ability to derive quantitative estimates of the rates of tectonic processes from topography is severely limited by the sparse data available to calibrate model parameters that describe erosive efficiency (Howard and Kerby, 1983; Stock and Montgomery, 1999; Snyder et al., 2000; Whipple et al., 2000b).

In this paper we develop a theory for the effect of spatially varying rock-uplift rates on the concavity of bedrock river profiles within the context of the detachment-limited unit-stream-power incision model (Howard et al., 1994). We demonstrate how analysis of stream profiles under conditions of nonuniform rock uplift allows for direct evaluation of model parameters. We test our model in a region of known variation in uplift rate within the Siwalik Hills of central Nepal. Rock-uplift rates across one anticline in the Siwalik Hills are well documented in a recent study of deformed Holocene terraces (Lavé and Avouac, 2000), vary in a systematic way across the fold, and appear to be constant throughout the Holocene. The anticline is developed in a region of uniform lithology and thus provides a nearly ideal location to examine the effects of spatially varying uplift rate on channel longitudinal profiles.

DETACHMENT-LIMITED STREAM POWER MODEL

Detachment-limited incision into bedrock is often modeled as a power-law function of contributing drainage area (a proxy for discharge) and channel gradient (Howard and Kerby, 1983; Howard, 1994). An equation for river profile evolution can be written as:

$$\frac{dz}{dt} = U(x, t) - KA^m S^n, \quad (1)$$

where dz/dt is the time rate of change of channel elevation, U is rock-uplift rate relative to a fixed base level, A is upstream drainage area, S is local channel gradient, K is a dimensional coefficient of erosion, and m and n are positive constants related to basin hydrology, hydraulic geometry, and erosion process (Howard et al., 1994; Whipple and Tucker, 1999; Whipple et al., 2000a). Under steady-state conditions ($dz/dt = 0$), with uniform U and K and constant m and n, equation (1) can be solved to yield an expression for equilibrium channel gradient:

$$S_e = (U/K)^{1/n} A^{-(m/n)}. \quad (2)$$

Equation 2 predicts a power-law relationship between channel gradient and drainage area often observed in natural landscapes, of the form $S = k_s A^{-\Theta}$ (e.g., Tarboton et al., 1991; Sklar and Dietrich, 1998), where the coefficient $(U/K)^{1/n}$ sets the channel steepness, k_s and the ratio m/n is the intrinsic channel concavity, which equals the actual concavity Θ only under conditions of uniform K, U, m, and n.

Relatively few field constraints exist on appropriate values for K, n, and m in various geologic, tectonic, and climatic regimes. Howard and Kerby (1983) demonstrated that historic incision rates in rapidly eroding badlands were adequately explained by a stream power model assuming incision rates linearly proportional to shear stress (i.e., $m = ⅓$, $n = ⅔$). Stock and Montgomery (1999) showed that, for a best-fit m and n (0.4 and 1, respectively), K varied over four orders of magnitude (10^{-3}–10^{-7} $m^{0.2}/yr$) depending on lithology and climate, and Snyder et al. (2000) demonstrated that K may also vary in concert with uplift rate (1–8 $\times$ 10^{-5} $m^{0.2}/yr$). Recent studies of historic bedrock incision along the Ukak River in Alaska have yielded results limiting n to significantly less than 1 ($n \approx 0.2$–0.6) and K (for $m = 0.4$, $n = 1$) to ~9×10^{-4} $m^{0.2}/yr$ (Whipple et al., 2000b).

Although individual values of the exponents m and n are difficult to obtain from natural field experiments, the ratio of m/n is expected to be independent of the erosion process (Whipple and Tucker, 1999) and thus is more easily estimated (Seidl and Dietrich, 1992). Theoretical considerations suggest that the ratio m/n should be in a narrow range between 0.35 and 0.6 (Whipple and Tucker, 1999), consistent with some empirical data (Howard and Kerby, 1983; Tarboton et al., 1991; Snyder et al., 2000). As pointed out by Whipple and Tucker (1999), a restricted range of the ratio m/n, however, does not neces-

*E-mail: ekirby@crustal.ucsb.edu.

sarily imply that channel concavities are likewise limited. Any spatial variation in K and/or U will strongly influence channel concavity (e.g., Sklar and Dietrich, 1998). Here we develop how spatial variations in rock-uplift rate affect the concavity of detachment-limited channels. We do not explicitly consider the potential role of sediment flux in influencing incision rates (Sklar and Dietrich, 1998). If present, its effect will be subsumed in our estimates of model parameters.

SPATIALLY VARIABLE ROCK-UPLIFT RATE

For the sake of brevity, we have restricted our analysis to a simple uplift function that yields a power-law gradient-area relationship,

$$U = U_0 x^{\alpha}, \tag{3}$$

where U_0 is the rock-uplift rate at the edge of the region of interest (taken here as the channel head) and α is a constant. Substituting equation 3 into equation 1, by using a well-known relationship between downstream distance and drainage area (Hack, 1957), where $A = k_a x^h$, and solving under the assumption of steady state yields an expression for equilibrium channel gradients of the form $S_e = k_s A^{-\Theta}$, where

$$k_s = (U_0/K)^{1/n} k_a^{-(\alpha/hn)} \quad \text{and} \tag{4}$$

$$\Theta = (m/n) - (\alpha/hn). \tag{5}$$

Equation 5 predicts that channels in regions where rock-uplift rate is increasing downstream ($\alpha > 0$) should have low concavities (or may even be convex upward), whereas those flowing toward regions of decreasing uplift rate ($\alpha < 0$) should have high concavities. When K is spatially uniform, equation 5 demonstrates that the slope exponent (n) can be directly estimated from the concavity of steady-state channels undergoing known downstream variations in rock-uplift rate.

SIWALIK HILLS FIELD AREA

The Siwalik Hills are a set of low ranges in the sub-Himalaya developed in the hanging wall of the Main Frontal thrust, the southernmost of a system of thrust faults in the Himalaya. The fault system disrupts Tertiary continental molasse of the Indo-Gangetic foredeep and currently marks the southern edge of active shortening in the Indo-Asian collision zone. Recent work on folded fluvial terraces along the Bagmati and Bakeya Rivers (Lavé and Avouac, 2000) (Fig. 1) demonstrates that (1) displacement on the main strand of the fault system locally absorbs ~20 mm/yr of shortening between India and Asia, (2) fold geometry is consistent with a model of fold growth above a ramp in the thrust, and (3) incision rates vary systematically across the fold and appear to have been nearly steady throughout the Holocene. Along the northern limb of the anticline, the vertical component of displacement increases in a nearly linear manner from ~5 mm/yr north of the fold to >15 mm/yr near the anticline crest (Lavé and Avouac, 2000). Rates then rapidly decrease to zero on the Indo-Gangetic plain. There also appears to be some variation in rock-uplift rate along strike; maximum inferred rates are ~12 mm/yr along the Bagmati River, and increase to ~17 mm/yr along the Bakeya River (Lavé and Avouac, 2000).

STREAM PROFILE ANALYSIS

We examined 22 channels in the vicinity of the Bagmati and Bakeya Rivers (Fig. 1). Our analysis follows the methods described by Snyder et al. (2000) and is detailed in the Data Repository[1]. Two of these channels (tributaries of the Bakeya and Bagmati, respectively) cross the anticline, spanning a range of rock-uplift rates from ~5 mm/yr to nearly 17 mm/yr, and provide the primary motivation for this study. Of the remaining 20 channels, 13 have their headwaters along the crest of the anticline and flow toward regions of decreasing uplift rate, and 7 flow parallel to the strike of the fold and to present-day uplift rate gradients (these strike-parallel streams were also studied by Hurtrez et al., 1999). We did not examine the Bagmati and Bakeya Rivers, because they have been thoroughly studied and appear to be gravel-bedded systems that respond to uplift of the anticline primarily by channel narrowing (Lavé and Avouac, 2000).

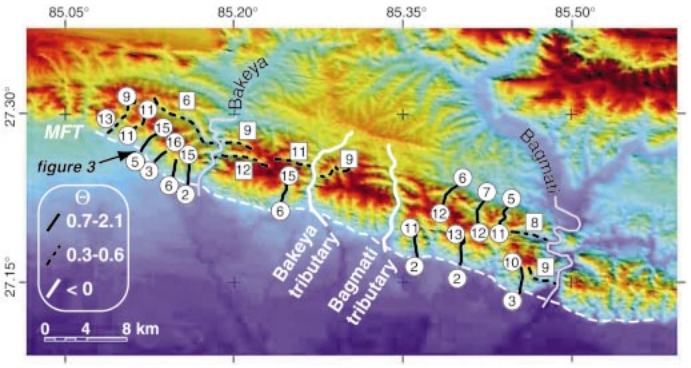

Figure 1. Concavity of channels draining Siwalik Hills in central Nepal. Background is shaded relief image derived from digital topography. Bagmati and Bakeya Rivers are shown in gray. Channels displaying concavities similar to expected range for conditions of uniform uplift are shown as dashed black lines, whereas channels with high concavities are shown as solid black lines. Channels with convex-upward ($\Theta < 0$) profiles are shown in white. Numbers refer to predicted erosion rates (in mm/yr) derived from calibrated channel incision rule (model parameters are $n = 1$, $m/n = 0.46$, $K = 1.5 \times 10^{-4}$ m$^{0.08}$/yr). Where erosion rates vary systematically along channel, rates are given at head and foot of channel (circles); where erosion rates are constant along channel, mean value is shown (squares). White dashed line represents inferred trace of Main Frontal thrust (MFT).

We observe pronounced variations in the concavity of channel profiles that depend on the position and orientation of the channel with respect to rock-uplift rate gradients across the anticline (Fig. 1), consistent with the predictions of equation 5. In particular, there are three groups of channel concavities. (1) Channels flowing parallel to the strike of the anticline display a narrow range of concavities between 0.4 and 0.5 (mean of 0.46; see footnote 1), in close agreement with theoretical predictions (Whipple and Tucker, 1999) and measurements (Snyder et al., 2000) of the concavity of equilibrium bedrock channels under conditions of uniform uplift and K. (2) Channels draining either flank of the anticline display consistently high concavities (Θ ranges from 0.7 to 2.1; see footnote 1), whereas (3) channels crossing the anticline from north to south display convex-upward ($\Theta < 0$) longitudinal profiles for ~7–9 km along the channels (Fig. 1). Because channels in this landscape are at or near steady state with respect to current climatic conditions (Lavé and Avouac, 2000), these differences appear to reflect the adjustment of channel gradient to variable rock-uplift rates.

Given that the pattern of rock uplift is best defined on the back (northern) limb of the Siwalik Hills anticline (Lavé and Avouac, 2000), we utilize the two main tributaries of the Bagmati and Bakeya Rivers that transect the anticline (Figs. 1 and 2) to calibrate a stream power incision model for this landscape. The vertical component of displacement increases linearly across the northern limb of the anticline, from ~4 mm/yr north of the fold to ~17 mm/yr at the crest (Lavé and Avouac, 2000), allowing us to determine the slope exponent (n) directly from the convexity of the channel profile ($\alpha = 1$ in equation 5).

[1]GSA Data Repository item 2001046, Topographic data and analytical methods, is available on request from Documents Secretary, GSA, P.O. Box 9140, Boulder, CO 80301-9140, editing@geosociety.org, or at www.geosociety.org/pubs/ft2001.htm.

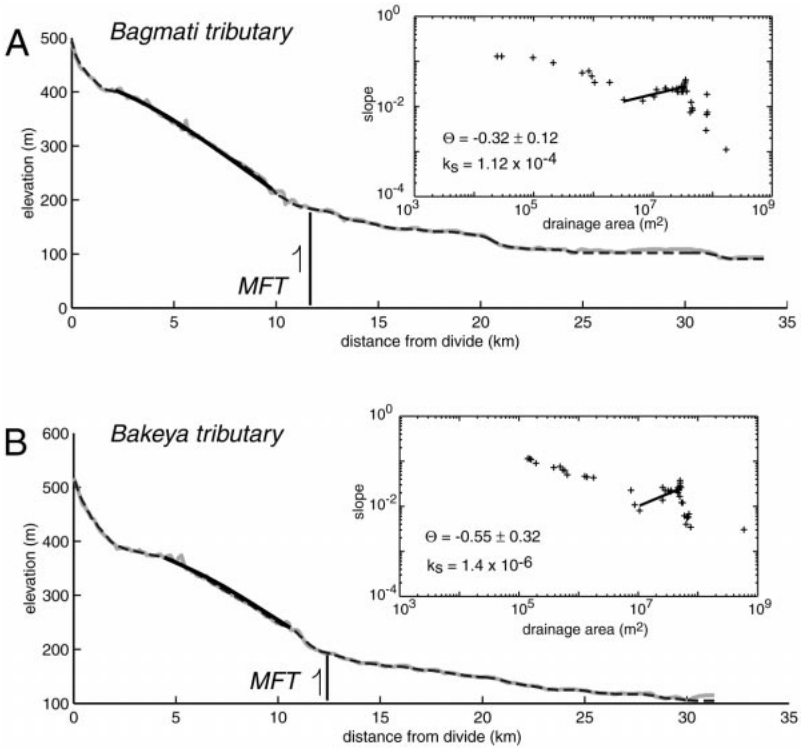

Figure 2. Channel longitudinal profiles for tributaries of Bagmati (A) and Bakeya (B) Rivers. See Figure 1 for location. Smoothed channel elevations are dashed lines (raw data in gray). Heavy black lines represent profile derived from best-fit regression of channel slope against drainage area. Insets are slope-area plots for each channel (see footnote 1); black lines are best-fit regression to channel segment. MFT is Main Frontal thrust.

We assume that the channels are in steady state, that the ratio m/n is ~0.46 (the mean of strike-parallel basins), and we utilized the Hack exponent derived for each river (see footnote 1). We estimate that the slope exponent (n) ranges from 0.6 to 0.9 (Fig. 2), consistent with incision rate nearly linear in basal shear stress ($n = 0.66$) or in unit stream power ($n = 1$) (Howard and Kerby, 1983; Whipple and Tucker, 1999). Our results are relatively insensitive to the choice of intrinsic concavity (m/n); varying m/n between 0.35 and 0.55 leads to a 0.08 variation in n.

In order to calibrate the erosion coefficient (K) for this landscape, we need to account for the additional uplift imparted by the advective component of the displacement field (e.g., Slingerland and Willett, 1999; Willett et al., 1999). The total or effective rock uplift (V_{eff}) is a function of channel gradient (S), such that:

$$V(x)_{\text{eff}} = V(x) + H(x)S, \quad (6)$$

where $V(x)$ and $H(x)$ are the vertical and horizontal components of the surface displacement field, respectively, and depend on the rate of slip on, and geometry of, the faults responsible for fold growth (e.g., Molnar, 1987). Because the channels utilized in our calibration have relatively gentle gradients (typically <10%), the horizontal component accounts for only a small (3%–5%) increase in uplift rate along the channel (see footnote 1 for details). It is likely, however, that the concavities of small, steep channels draining the flanks of the anticline are significantly affected by the advective component of the displacement field.

We calculate the coefficient of erosion, K, for each model of n (Table 1), utilizing equation 1. To evaluate the range of variability imparted by along-strike variations in rock-uplift rates, we calculated K for uplift patterns derived from each transect of Lavé and Avouac (2000) (Table 1). If erosion is linear in stream power ($n = 1$), values of K range from $\sim 1.5 \times 10^{-4}$ to $\sim 1.6 \times 10^{-4}$ $m^{0.08}$/yr, whereas if erosion is linear in shear stress ($n = ⅔$), values of K range from $\sim 6.0 \times 10^{-4}$ to $\sim 6.9 \times 10^{-4}$ $m^{0.05}$/yr (Table 1).

MODELING EROSION RATES

The power of this approach lies in its ability to quantify the magnitude and spatial distribution of erosion rates in the Siwalik Hills. We

TABLE 1. SIWALIK HILLS INCISION MODEL PARAMETERS

Principal channel	n ($\alpha = 1$)	K ($m^{0.08}$/yr) ($n = 1$, $m/n = 0.46$)	K ($m^{0.05}$/yr) ($n = 0.66$, $m/n = 0.46$)	K ($m^{0.2}$/yr) ($n = 1$, $m/n = 0.4$)*
U(x) = 4–18 mm/yr				
Bakeya tributary	0.59	1.64×10^{-4} ($\pm 2.54 \times 10^{-5}$)	6.85×10^{-4} ($\pm 1.50 \times 10^{-4}$)	4.68×10^{-4} ($\pm 7.76 \times 10^{-5}$)
Bagmati tributary	0.88	1.54×10^{-4} ($\pm 2.95 \times 10^{-5}$)	6.39×10^{-4} ($\pm 1.73 \times 10^{-4}$)	4.27×10^{-4} ($\pm 8.91 \times 10^{-5}$)
U(x) = 6–12 mm/yr				
Bakeya tributary	0.59	1.47×10^{-4} ($\pm 2.78 \times 10^{-5}$)	6.02×10^{-4} ($\pm 7.10 \times 10^{-5}$)	4.19×10^{-4} ($\pm 7.36 \times 10^{-5}$)
Bagmati tributary	0.88	1.48×10^{-4} ($\pm 2.98 \times 10^{-5}$)	5.95×10^{-4} ($\pm 6.00 \times 10^{-5}$)	4.08×10^{-4} ($\pm 7.18 \times 10^{-5}$)
mean		***1.54 × 10⁻⁴***	***6.30 × 10⁻⁴***	***4.32 × 10⁻⁴***
2σ		***2.90 × 10⁻⁵***	***1.27 × 10⁻⁴***	***8.13 × 10⁻⁵***

Note: K was calculated for each data point along the channel (see footnote 1). Mean values and standard deviations (parentheses) are given. Uncertainties on the global means reflect a Monte Carlo propagation of uncertainties.

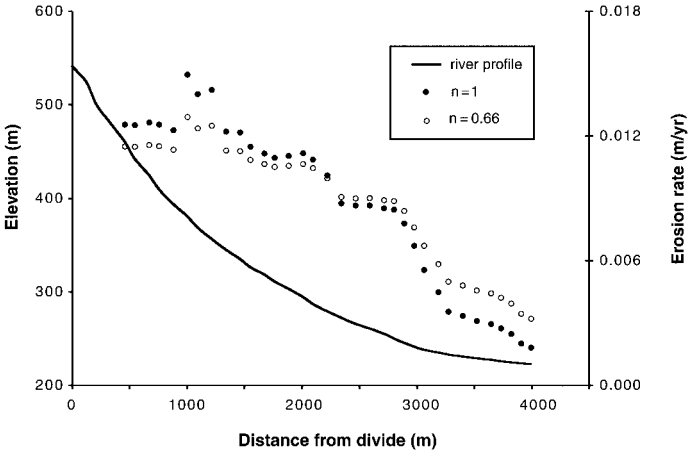

Figure 3. Predicted erosion rates along small channel draining southern flank of anticline (see Figure 1 for location). Erosion rates modeled with calibrated incision rule decrease rapidly downstream over a few kilometers between anticline crest and foreland, consistent with rapidly decreasing rock uplift near trace of Main Frontal thrust. Open symbols represent modeled rates for $n = 0.66$; closed symbols represent rates for $n = 1$.

utilized calibrated parameters in the stream power incision model to predict erosion rates along a number of the small channels draining the front and back limbs of the Siwalik Hills anticline. Modeled erosion rates, for either $n = ⅔$ or $n = 1$, along channels draining the northern and southern limbs of the anticline generally decrease downstream in a nearly linear fashion, whereas erosion rates along channels oriented parallel to strike are nearly constant (Figs. 1 and 3). Furthermore, the magnitudes of modeled erosion rates closely reproduce the expected range of rock-uplift rates (Hurtrez et al., 1999; Lavé and Avouac, 2000) across the flanks of the anticline (Figs. 1 and 3). This test confirms the utility of equation 3 for calibrating the channel incision model—model parameters are portable to streams of different sizes undergoing different rock-uplift patterns.

Although interpretation of erosion-rate patterns in terms of variations in deformation along the anticline is complicated by the need to deconvolve the role of the horizontal component of rock advection, especially on the gradients of small, steep channels (equation 6; Slingerland and Willett, 1999; Willett et al., 1999), insofar as erosion rates are in balance with the tectonic influx of material, we can, in principle, predict, and then invert erosion rates in this landscape for deformation rates above active structures.

DISCUSSION AND CONCLUSIONS

Our analysis of stream gradients in the Siwalik Hills suggests that a stream power incision model provides a promising means of evaluating channel response to spatial variations in rock-uplift rate. We find that the dependence of incision rate on channel gradient in this landscape is consistent with erosion linearly proportional to either basal shear stress ($n = ⅔$) or stream power ($n = 1$), as one might expect for weakly consolidated substrate (Howard and Kerby, 1983). To facilitate comparison with published estimates of stream power incision parameters, we calculate K for values $m = 0.4$, $n = 1$ (Stock and Montgomery, 1999). The resultant estimates yield a mean of $\sim 4.3 \times 10^{-4}$ $m^{0.2}$/yr (Table 1). Thus, although incision rates are high, the erosion coefficient is within the range of published estimates for weak, easily erodible rock in regions with abundant precipitation (Stock and Montgomery, 1999; Whipple et al., 2000b).

Our results further indicate that rock-uplift rate exerts a fundamental control on channel gradient in the Siwalik Hills and that systematic differences in channel concavity reflect pronounced spatial variations in rock-uplift rate across the fold. It is interesting that erosion rates derived from the calibrated stream-power parameters (Fig. 1) yield rock-uplift rates along the southern limb of the anticline remarkably consistent with those modeled by Hurtrez et al. (1999) from the local relief (measured over length scales <600 m).

This study illustrates the potential of stream-gradient analysis as a quantitative method for extracting information on the rates and spatial distribution of rock uplift from digital topographic data. Systematic variations in channel gradient and, particularly, concavity can highlight regions of underlying variation in rock-uplift rate and place direct constraints on the geometry and distribution of active structures (e.g., Molnar, 1987). Such analysis is subject to complications introduced by variations in lithology, by transient conditions, by glacial erosion, and possibly by downstream variations in sediment flux and must be applied with caution. However, it appears that we now have the ability to predict erosion rates in the Siwalik Hills directly from topographic analyses, affording the opportunity to assess the spatial variability of active deformation within the Himalayan foreland from landscape response.

ACKNOWLEDGMENTS

We thank Simon Brocklehurst, Dan Miller, Noah Snyder, and Greg Tucker for discussions on various aspects of this study and Peter Molnar and Doug Burbank for comments on an early draft. Dave Montgomery and Rudy Slingerland provided insightful reviews. Work was supported by National Science Foundation grants EAR-9614970 and EAR-9725723.

REFERENCES CITED

Hack, J.T., 1957, Studies of longitudinal stream profiles in Virginia and Maryland: U.S. Geological Survey Professional Paper 294-B, p. 45–97.

Howard, A.D., 1994, A detachment-limited model of drainage basin evolution: Water Resources Research, v. 30, p. 2261–2285.

Howard, A.D., and Kerby, G., 1983, Channel changes in badlands: Geological Society of America Bulletin, v. 94, p. 739–752.

Howard, A.D., Seidl, M.A., and Dietrich, W.E., 1994, Modeling fluvial erosion on regional to continental scales: Journal of Geophysical Research, v. 99, p. 13 971–13 986.

Hurtrez, J.-E., Lucazeau, F., Lavé, J., and Avouac, J.-P., 1999, Investigation of the relationship between basin morphology, tectonic uplift, and denudation from the study of an active fold belt in the Siwalik Hills, central Nepal: Journal of Geophysical Research, v. 104, p. 12 779–12 796.

Lavé, J., and Avouac, J.-P., 2000, Active folding of fluvial terraces across the Siwalik Hills, Himalayas of central Nepal: Journal of Geophysical Research, v. 105, p. 5735–5770.

Molnar, P., 1987, Inversion of profiles of uplift rates for the geometry of dip-slip faults at depth, with examples from the Alps and Himalaya: Annales Geophysicae, v. 5B, p. 663–670.

Seidl, M.A., and Dietrich, W.E., 1992, The problem of channel erosion into bedrock: Catena, Supplement, v. 23, p. 101–124.

Sklar, L., and Dietrich, W.E., 1998, River longitudinal profiles and bedrock incision models: Stream power and the influence of sediment supply, *in* Tinkler, K.J., and Wohl, E.E., eds., Rivers over rock: Fluvial processes in bedrock channels: American Geophysical Union Geophysical Monograph 107, p. 237–260.

Slingerland, R., and Willett, S.D., 1999, Systematic slope-area functions in the central range of Taiwan may imply topographic unsteadiness: Eos (Transactions, American Geophysical Union), v. 80, p. 448.

Snyder, N.P., Whipple, K.X., Tucker, G.E., and Merritts, D.J., 2000, Landscape response to tectonic forcing: Digital elevation model analysis of stream profiles in the Mendocino triple junction region, northern California: Geological Society of America Bulletin, v. 112, p. 1250–1263.

Stock, J.D., and Montgomery, D.R., 1999, Geologic constraints on bedrock river incision using the stream power law: Journal of Geophysical Research, v. 104, p. 4983–4993.

Tarboton, D.G., Bras, R.L., and Rodriguez-Iturbe, I., 1991, On the extraction of channel networks from digital elevation data: Hydrological Processes, v. 5, p. 81–100.

Tinkler, K.J., and Wohl, E.E., editors, 1998, Rivers over rock: Fluvial processes in bedrock channels: American Geophysical Union Geophysical Monograph 107, 323 p.

Whipple, K.X., and Tucker, G.E., 1999, Dynamics of the stream-power river incision model: Implications for height limits of mountain ranges, landscape response timescales, and research needs: Journal of Geophysical Research, v. 104, p. 17 661–17 674.

Whipple, K.X., Kirby, E., and Brocklehurst, S.H., 1999, Geomorphic limits to climate-induced increases in topographic relief: Nature, v. 401, p. 39–43.

Whipple, K.X., Hancock, G.S., and Anderson, R.S., 2000a, River incision into bedrock: Mechanics and relative efficacy of plucking, abrasion, and cavitation: Geological Society of America Bulletin, v. 112, p. 490–503.

Whipple, K.X., Snyder, N.P., and Dollenmayer, K., 2000b, Rates and processes of bedrock incision by the Upper Ukak River since the 1912 Novarupta ash flow in the Valley of Ten Thousand Smokes, Alaska: Geology, v. 28, p. 835–838.

Willett, S.D., Hovius, N., and Slingerland, R., 1999, The effects of horizontal motion on topography and patterns of exhumation in convergent mountain belts: Eos (Transactions, American Geophysical Union), v. 80, p. 1033.

Manuscript received August 18, 2000
Revised manuscript received January 3, 2001
Manuscript accepted January 21, 2001

Printed in USA

Data Repository

Quantifying differential rock-uplift rates via stream profile analysis

Eric Kirby and Kelin Whipple
Department of Earth, Atmospheric and Planetary Sciences, Massachusetts Institute of Technology, Cambridge, Massachusetts, 02139, USA; email: ekirby@mit.edu

Analytical Methods

Channel elevations and upstream drainage areas were extracted from digital topographic data with a nominal resolution of 90 m (DTED data source, described in Fielding et al., 1994). We utilized standard flow-routing algorithms in ARCINFO to generate channel networks by filling local minima in the data. We then sampled elevations along the flow paths from the unprocessed DEM and removed spikes along the channel profiles by not allowing any pixel to be higher than the pixel immediately upstream. We smoothed the resultant data using a moving average of 10 pixels (arbitrarily chosen to capture the > 1 km features of the channel profile while reducing scatter) and calculated channel gradients at 10m vertical intervals along the profile (e.g., Snyder et al., 2000) (Fig. 2). This method is comparable to digitizing gradients from topographic maps. Regression of gradients against upstream area yielded estimates of the concavity and steepness indices (Θ and k_s, respectively), while regression of drainage area against streamwise distance yielded estimates of h (Table DR-1). All regressions excluded data from hillslopes (Montgomery and Foufoula-Georgiou, 1993; Snyder et al., 2000) and from alluviated sections of the channels on either side of the anticline.

Incision Model Calibration

In order to calibrate a stream power incision model along a channel experiencing a range of rock uplift rates above a developing fault-bend fold, we need to consider the total displacement field at each point along the channel. Consider a fault whose dip, relative to the horizontal, is given by Θ_d and with displacement rate D. The vertical component of deformation is given by:

$$V(x) = D\sin\Theta_d \qquad \text{(A1)}$$

and the horizontal component by:

$$H(x) = D\cos\Theta_d \qquad \text{(A2a)}$$

or

$$H(x) = V(x)\cos\Theta_d/\sin\Theta_d \qquad \text{(A2b).}$$

The horizontal component of displacement imparts an effective ‘uplift’ component that depends on the local gradient of the channel, S, such that:

$$H(x)_v = H(x)S = V(x)S/\tan\Theta_d \qquad \text{(A3).}$$

Note that *S* is positive if the channel flows in the same direction as the displacement vector and is negative if opposite. The effect will thus be to increase the 'uplift' rate on channels flowing in the direction of displacement and decrease 'uplift' rate on those opposed to it. The total effective vertical displacement felt by any point on the channel is simply the sum of these components:

$$V(x)_{eff} = V(x)\left(1 + S/\tan\Theta_d\right) \qquad \text{(A4).}$$

Thus, given a priori knowledge of the fault geometry, one can in principle extract the displacement rate, *D*, across a fault-bend fold from the steady-state erosion rate, ε:

$$D = \frac{\varepsilon}{(\sin\Theta_d + S\cos\Theta_d)} \qquad \text{(A5).}$$

Lavé and Avouac (2000) documented a correspondence between bedding dip angles and rock uplift profiles inferred from deformed fluvial terraces along the Bagmati and Bakeya rivers, suggesting that a model of fault-bend folding adequately described the deformation field across the Siwalik anticline. Furthermore, these authors demonstrated that the horizontal component of displacement accounts for a negligible difference (<1%) in effective uplift rate felt by these low gradient channels. In order to model the distribution of deformation along the tributary streams in this study, we utilize the geometry of bedding dip angles measured by Lavé and Avouac (2000) and a displacement rate of 21 mm/yr (Fig. DR-2). We also consider the effect of the horizontal component of displacement; although the tributaries we examine are somewhat steeper than the Bagmati and Bakeya rivers, the additional component of 'uplift' felt by these rivers is on the order of 3-5% (Fig. DR-2). Note that in both deformation models, the effective vertical displacement increases linearly along the northern limb of the fold (Fig. DR-2). Consequently, the additional component of displacement (equation A3) does not significantly change our estimate of the slope exponent *n*.

We calculate the erosion coefficient *K* as a function of downstream distance using equation (2). We combine the effective vertical displacement patterns described above (Fig. DR-2) with drainage areas extracted from the digital topography and the local channel gradient. The difference in displacement patterns between the Bagmati and Bakeya rivers (Fig. DR-2) presents the greatest source of uncertainty in our calculation. Given that the tributaries are located between these two transects (Figure 1), we calculate *K* for each displacement pattern and take the mean of these values (Table 1). Standard

deviations are calculated for each estimate of *K* (Table 1), and these are incorporated into a Monte Carlo estimation of uncertainties on the global means. Because the gradients on the channels we utilized in our calibration are relatively gentle (typically < 10%), the influence of horizontal advection effective 'uplift rate' along the channel is minor; estimates of mean *K* shift by ~8% when advection is not considered.

List of Figure Captions

Figure DR-1. Index map of channels examined in the Siwalik Hills. Background is a grayscale image of Fig. 1. Numbers refer to channel data in Table DR-1.

Figure DR-2. Vertical displacement patterns above the Main Frontal Thrust for the Bakeya (a) and Bagmati (b) transects. Rates were derived using bedding dip orientations from Lavé and Avouac (2000). Open circles represent the vertical component of deformation derived for a constant shortening rate of 21 mm/yr. Filled circles represent the total effective vertical component derived from equation (A4) and utilized in calibration of the erosion coefficient *K*.

References Cited

Fielding, E.J., Isacks, B.L., Barazangi, M., and Duncan, C., 1994, How flat is Tibet?: Geology, v. 22, p. 163-167.

Montgomery, D.R., and Foufoula-Georgiou, E., 1993, Channel network source representation using digital elevation models: Water Resources Research, v. 29, p. 1178-1191.

Snyder, N.P., Whipple, K.X., Tucker, G.E., and Merritts, D.J., 2000, Landscape response to tectonic forcing: Digital elevation model analysis of stream profiles in the Mendocino triple junction region, northern California: Geological Society of America Bulletin, v. 112, p. 1250-1263.

Data Repository Table 1. Topographic characteristics of channels in the Siwalik Hills

Principal channel	A_{min} (m^2)	A_{max} (m^2)	$\Theta \pm 2\sigma$ (Θ = 0.46)	k_s	$h \pm 2\sigma$	E^* (mm/yr) (n = 0.66)	E^* (mm/yr) (n = 1)	$E^\dagger$ (mm/yr) (n = 0.66)	$E^\dagger$ (mm/yr) (n = 1)
akeya tributary	9×10^6	5×10^7	-0.55 ± 0.32	59	.68 ± 0.13				
agmati tributar	3×10^6	3.5×10^7	-0.32 ± 0.12	55	.46 ± 0.10				
1	1×10^6	1×10^7	0.30 ± 0.10[§]	60	.26 ± 0.12	8-11 (0.80)	8-11 (0.81)	9-12 (0.45)	9-13 (0.45)
2	1×10^6	4×10^6	0.53 ± 0.20[§]	70	.94 ± 0.03	[10.7]	[11.3]	[10.4]	[10.8]
3	2×10^6	5×10^6	1.30 ± 0.32	75	.64 ± 0.05	12-7 (0.95)	11-8 (0.94)	13-6 (0.82)	15-5 (0.80)
4	1×10^6	3×10^6	1.10 ± 0.20	88	.15 ± 0.23	9-6 (0.83)	9-5 (0.81)	13-5 (0.85)	15-3 (0.82)
5	5×10^5	3×10^6	1.00 ± 0.18	58	.04 ± 0.05	13-6 (0.90)	14-5 (0.87)	13-7 (0.64)	16-6 (0.62)
6	1.5×10^6	3×10^6	2.10 ± 0.61	51	.54 ± 0.04	12-7 (0.93)	14-5 (0.91)	13-3 (0.86)	15-2 (0.81)
7	2×10^6	1×10^7	1.30 ± 0.33	81	.05 ± 0.10	10-4 (0.86)	11-3 (0.82)	13-7 (0.20)	15-6 (0.21)
8	1×10^6	4×10^6	1.10 ± 0.31	56	.96 ± 0.07	15-9 (0.89)	18-9 (0.88)	11-3 (0.86)	11-2 (0.84)
9	2×10^6	7×10^6	0.99 ± 0.14	68	.73 ± 0.04	12-8 (0.91)	14-7 (0.90)	12-3 (0.82)	13-2 (0.80)
10	5×10^5	4×10^6	1.20 ± 0.22	48	.90 ± 0.03	15-7 (0.79)	18-6 (0.76)	10-4 (0.66)	10-3 (0.65)
11	1×10^6	8×10^6	0.74 ± 0.16	67	.75 ± 0.25	12-9 (0.98)	13-9 (0.98)	11-7 (0.68)	12-6 (0.66)
12	1×10^6	4×10^6	1.40 ± 0.28	74	.84 ± 0.20	8-5 (0.96)	8-4 (0.96)	11-8 (0.64)	12-7 (0.64)
13	9×10^5	5×10^6	0.87 ± 0.25	49	.06 ± 0.16	10-7 (0.74)	10-6 (0.72)	11-6 (0.73)	11-5 (0.72)
14	4×10^5	5×10^6	0.50 ± 0.29	51	.01 ± 0.54	[8.7]	[8.3]	[8.6]	[8.1]
15	5×10^5	1×10^7	0.47 ± 0.16	59	.58 ± 0.10	[9.0]	[8.6]	[9.3]	[9.2]
16	1×10^6	7×10^6	0.48 ± 0.14	60	.64 ± 0.17	[9.0]	[8.6]	[9.5]	[9.4]
17	6×10^5	2×10^6	0.51 ± 0.42	72	.39 ± 0.70	[11.0]	[11.7]	[10.6]	[11.1]
18	1×10^6	1×10^7	0.44 ± 0.22	72	.14 ± 0.05	[10.8]	[11.3]	[10.9]	[11.8]
19	7×10^5	2.5×10^6	0.34 ± 0.34	63	.28 ± 0.09	[10.2]	[10.5]	[9.4]	[9.2]
20	1×10^6	1.5×10^7	0.51 ± 0.22	35	.35 ± 0.07	[6.5]	[5.3]	[6.7]	[5.5]
mean (3-10)			***1.26 ± 0.37***	***66***					
mean (11-13)			***1.01 ± 0.31***	***63***					
mean (3-13)			***1.19 ± 0.38***	***65***					
mean (14-20)			***0.46 ± 0.14***	***59***					

* Erosion rate calculated using channel gradients inferred from Θ and k_s. Where rates vary along a channel, values represent rates at A_{min} and A_{max}, respectively. Correlation coefficient of linear regression (R^2) shown in parentheses. Where rates are invariant along a channel, number brackets represents the mean erosion rate.

† Same as in the first footnote, but calculated by using channel gradient sampled at 10 m intervals.

§ Excluded from mean.

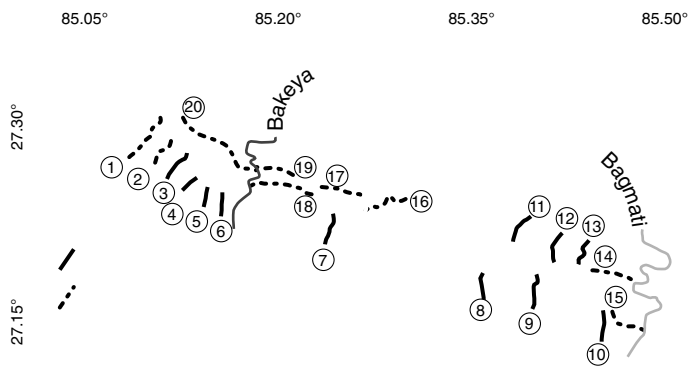

Kirby and Whipple, Figure DR-1

a.

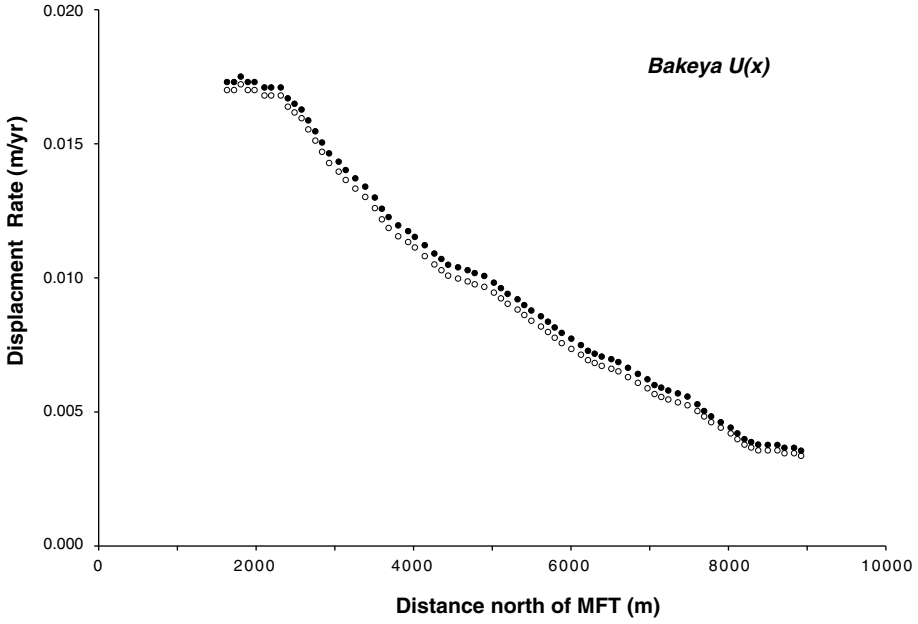

b.

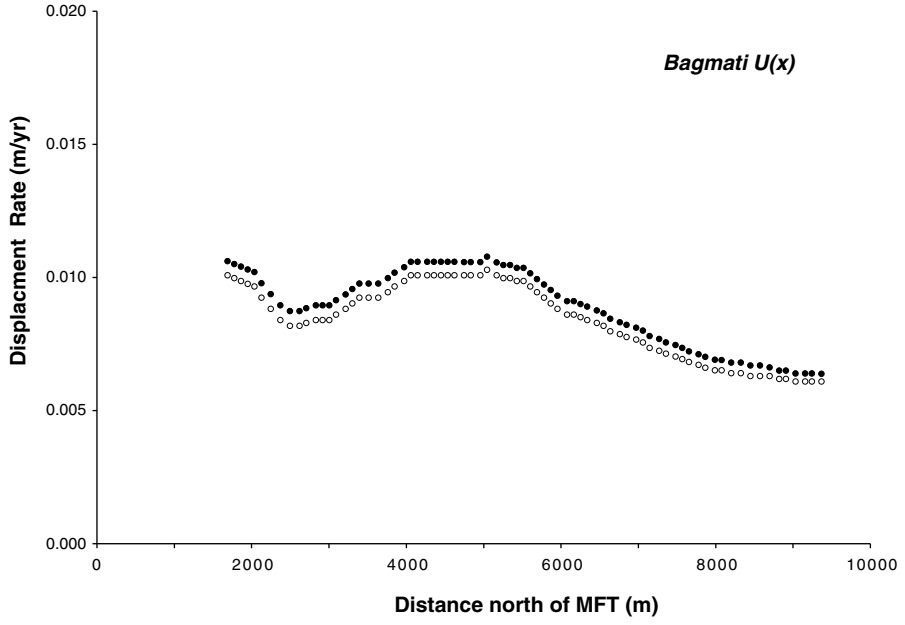

Kirby and Whipple - Figure DR-2